

# Study on the Drawing Behavior of Poly(L-Lactide) to Obtain High-Strength Fibers

A. R. POSTEMA and A. J. PENNINGS, *Department of Polymer Chemistry, University of Groningen, Nijenborgh 16, 9747 AG Groningen, The Netherlands*

## Synopsis

The tensile drawing behavior of poly(L-lactide) has been studied in order to obtain high strength fibers. Elongational viscosity measurements indicated that the hot drawing can take place in two temperature regions with different activation energies. Up to 180°C, the deformation proceeds in the semicrystalline state of the polymer having an activation energy of 15–28 kJ/mol, presumably by shear deformation. In the range of 180–190°C, the deformation proceeds in the liquid state of the polymer having an activation energy of 145–165 kJ/mol, leading to a semicrystalline state by strain hardening after displacement of topological defects. By using high deformation rates during drawing in a temperature gradient (tube drawing), the deformation will principally proceed in the semicrystalline region and inhomogeneous draw will take place leading to inferior fiber properties, unless the deformation rate and drawing temperature are strictly adjusted. Homogeneous drawing can be achieved by applying low deformation rates so that the deformation may take place in the liquid state of the polymer in which individual chains can be easily aligned and topological defects can be removed. Poly(L-lactide) fibers with tensile strengths of 2.3 GPa have been produced in this way.

## INTRODUCTION

Because of its biocompatibility poly(L-lactide) (PLLA) has been widely studied for biomedical applications such as body absorbable sutures.<sup>1–9</sup> High-strength fibers (tenacity > 1 GPa) may find applications as a small-sized suture in microsurgery or become useful in the field of composite materials.<sup>10–12</sup>

PLLA fibers ( $\bar{M}_v = 5\text{--}6 \times 10^5$ ) with tenacity of 1–1.2 GPa could be produced by dry spinning/hot drawing of PLLA solutions in toluene (poor solvent) and chloroform (good solvent), respectively.<sup>4,5</sup> Leenslag and Pennings<sup>9</sup> showed that, by using higher molecular weight PLLA, obtained by bulk polymerization of L-lactide at relative low temperatures (100–110°C), improved mechanical properties could be obtained by spinning from binary solvent mixtures near the  $\theta$  conditions in which the PLLA adopts an interrupted helical conformation. PLLA fibers with a tenacity of 2.1 GPa and a Young's modulus of 16 GPa could be obtained by dry-spinning PLLA from a chloroform/toluene (40/60 v/v) mixture and subsequent hot drawing at 204°C.

Not only the molecular weight and the solvent composition but also several other factors such as the PLLA concentration in the spinning solution, the

drawing temperature, the molecular weight distribution, and the fiber diameter were found to affect the ultimate fiber properties.

In the hot-drawing process, PLLA can exhibit an  $\alpha, \beta$  crystal transition. Synchrotron radiation studies by Hoogsteen et al.<sup>13</sup> indicated that this  $\beta$ -form (assumed a 3/1 helix), if present, probably is the load-bearing structure in the PLLA fibers.

In the present study, the hot-drawing process of PLLA has been examined in more detail. A dependence of the drawing process on the molecular weight and the molecular weight distribution was already recognized by Capaccio and co-workers<sup>14-17</sup> for polyethylene and polypropylene fibers. The study of Leenslag and Pennings<sup>9</sup> showed that using PLLA samples with narrow molecular weight distribution (obtained by fractionation) gave fibers with properties inferior to fibers obtained by using a broad molecular weight distribution. We have investigated the origin of these inferior properties and how to vary the drawing conditions in order to obtain equal or even better ultimate mechanical properties. To be sure that topological defects like knots,<sup>18</sup> possibly introduced during fractionation, could not affect the results of our study, we have used a PLLA sample which showed the same drawing characteristics as the fractionated sample of Leenslag and Pennings<sup>9</sup> and which is to be expected to have a narrow molecular weight distribution.<sup>19</sup>

It will be shown that using high deformation rates/entrance velocities during tube drawing, the deformation process will take place in the semicrystalline state of the PLLA leading to inhomogeneous drawing and inferior fiber properties. Homogeneous drawing takes place if low deformation rates/entrance velocities are used and the drawing takes place in the liquid state of the PLLA, so that individual chains can be easily aligned and topological defects can be removed, leading to fibers with a tensile strength of 2.3 GPa.

## EXPERIMENTAL

### Preparation of the Polymer

Poly(L-lactide) with  $\bar{M}_v = 9.1 \times 10^5$  ( $\Delta H_m = 52.2$  J/g,  $T_m = 189.5^\circ\text{C}$ ) was synthesized<sup>19</sup> by polymerization of purified (by recrystallization from toluene (Merck, distilled from sodium) under nitrogen atmosphere) L-lactide (C.C.A., Gorinchem, The Netherlands) in vacuum-sealed ( $10^{-7}$  Torr) silanized glass ampoules at  $110^\circ\text{C}$ . The time of polymerization was 210 h. Stannous-2-ethylhexanoate (Sigma Chemical Corp., U.S.A.) was used as a catalyst (0.005–0.045 wt %). The viscosity-average mol weight  $\bar{M}_v$  of the sample was estimated from the intrinsic viscosity  $[\eta]$  in chloroform at  $25^\circ\text{C}$  according to the relationship<sup>20</sup>:  $[\eta] = 5.45 \times 10^{-4} \bar{M}_v^{0.73}$ .

### Preparation of the Spinning Solutions

The spinning solutions were prepared by dissolving 2 g PLLA in 25 mL chloroform (Merck) at  $22^\circ\text{C}$ . After 1 week, the excess chloroform was evaporated to 20 mL chloroform and 30 mL toluene (Merck, distilled from sodium) was added to the solutions without mechanical stirring, and the solutions were homogenized by standing for 2 weeks. It was not possible to dissolve the polymer directly into the chloroform/toluene mixture.

### Dry Spinning of the PLLA Gel

In a piston-cylinder apparatus the 4% (m/v) PLLA solution was conditioned at 70°C for 3 h. The solutions were extruded at 60°C through a stainless-steel, conical die (entrance-angle 43°, length 23 mm, and exit diameter 0.25 mm) and collected (at 20–22°C) on sand-blasted glass bobbins without applying additional stress to the extrudate. The distance between die and bobbin was 6.5 cm. The extrusion rate was 3 m/min. The as-spun fibers were dried on the bobbins at room temperature until constant weight was reached (usually about 40 h).

### Hot Drawing of the PLLA Fibers

The hot-drawing experiments were carried out in a heated, double-walled glass tube (length 0.6 m) as described previously,<sup>5</sup> at different temperatures and different entrance velocities, in a nitrogen (dried over Sicapent) atmosphere. The accuracy of the rotational velocities of the bobbins in the drawing apparatus was within 1%.

### Characterization of the Fibers

An ISI-DS-130 scanning electron microscope, operated at 5–10 kV was used to study the necking behavior of the PLLA filaments. Mechanical properties of the fibers were determined at room temperature using an Instron (4301) tensile tester, equipped with a 10N load-cell, at a cross-head speed of 12 mm/min. The length of the specimen was 25 mm. Cross sections of the fibers were calculated from the fiber weight and length, assuming a value of 1290 kg/m<sup>3</sup> for the density of the fiber.<sup>21</sup> All the tensile properties to be presented are the average values of at least five tests.

### Dynamometer

To study the effect of temperature and deformation rate on the hot drawing of PLLA fibers, isothermal drawing experiments were carried out in a dynamometer<sup>22</sup> in which the samples could be elongated at constant rate of deformation. The motor of the dynamometer (Maxon DC, type 2332.910, Interelectric A.G., Sachseln, Germany) was headed with an exponential voltage generator (equipped with a log/antilog amplifier type 755N, Analog devices, Norwood, U.S.A.) causing an exponentially increasing cross-head speed, resulting in a constant deformation rate of the fiber. The load cell (Statham Instruments, Model UC3 equipped with a UL5 load-cell accessory) has a measuring range of 0–200 g. Five fixed deformation rates were available in the range from  $0.444 \times 10^{-3}$  to  $8.889 \times 10^{-3}$  s<sup>-1</sup>. In order to prevent slippage, the fiber was clamped between two, with screws connected, sand-blasted plates (7 × 5 mm). The initial length of the fibers was 15 mm. The temperature throughout the glass vessel of the dynamometer was constant within 0.5°C. The temperature was measured in the direct vicinity of the sample by means of a resistor thermometer (Pt100). To prevent degradation, dry nitrogen was allowed to flow through the glass vessel at a moderate rate. To get isothermal conditions established, it was necessary to wait sometime

after clamping the fibers, before the elongation was started. A period of 15 min was found to be sufficient to obtain good reproducibility.

## RESULTS AND DISCUSSION

After spinning the PLLA solutions, fibers with a porous texture were obtained (Fig. 1). This porosity seems to be necessary in order to obtain homogeneous deformation during hot drawing.<sup>23</sup> At first we investigated the influence of the drawing temperature in the hot-drawing process by applying an entrance velocity of 6.25 cm/min. In Figure 2 the tensile strength of the PLLA fibers after drawing to the maximum draw ratio at different drawing temperatures is presented. A maximum in the tensile strength of 1.6 GPa is obtained after drawing at a temperature of 214°C and a maximum draw ratio of 13 was attained. During verification of the draw ratio we observed a disagreement between the draw ratio calculated from the length increase and the draw ratio calculated from the reduction of mass per unit length during hot drawing. The length draw ratio (LDR) is calculated from the entrance and exit velocities (Fig. 3) during hot drawing:

$$\text{LDR} = \frac{V(\text{exit})}{V(\text{entrance})} \quad (1)$$

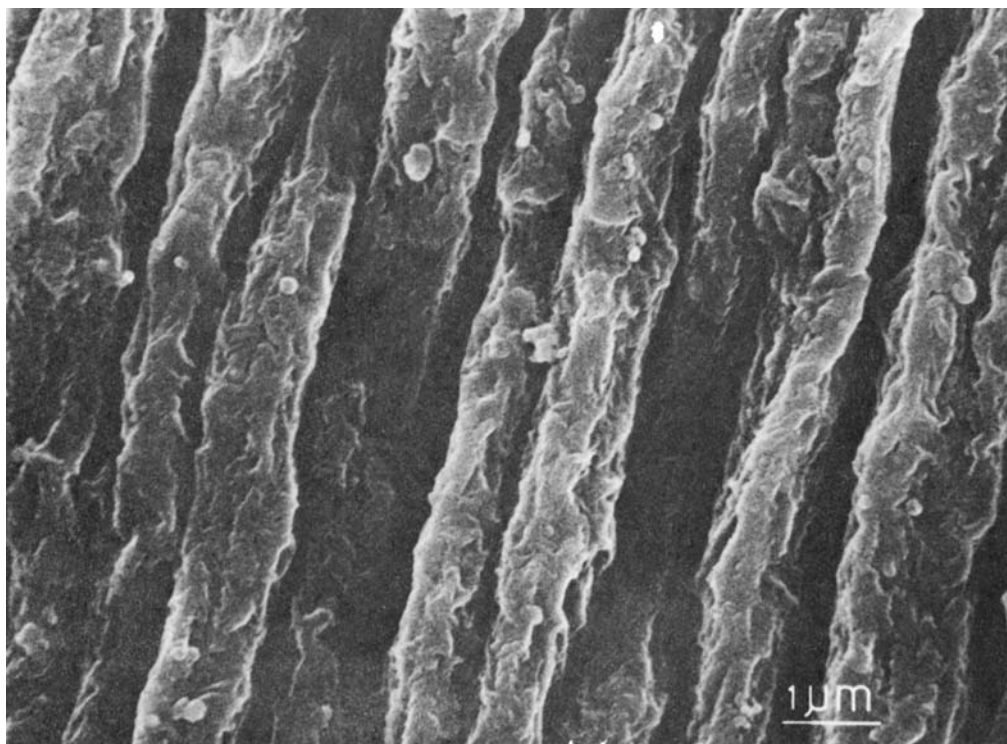


Fig. 1. SEM of an as-spun PLLA fiber, produced from a 4% (w/v) PLLA solution in chloroform/toluene 40/60 (v/v) at 60°C, showing a highly porous surface texture.

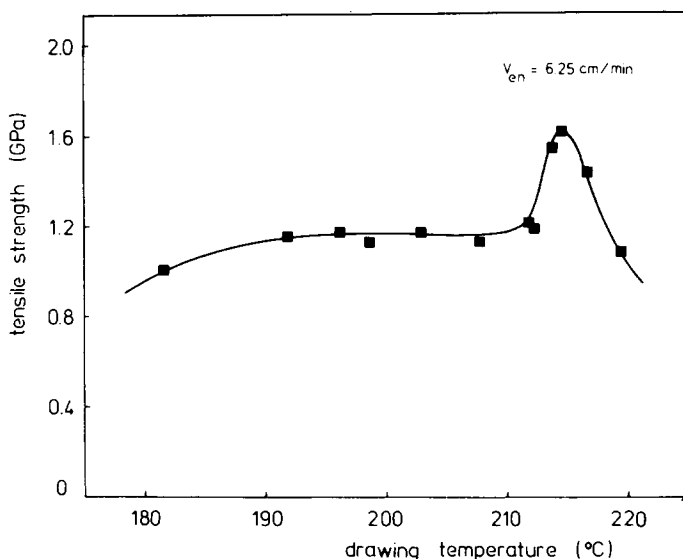


Fig. 2. Tensile strength of PLLA fibers hot-drawn at different temperatures to the maximal draw ratio using an entrance velocity of 6.25 cm/min in a tube-drawing process.

The mass draw ratio (MDR) is calculated from the mass of 1 m fiber before and after drawing:

$$\text{MDR} = \frac{\text{mass undrawn sample per unit length}}{\text{mass drawn sample per unit length}} \quad (2)$$

In case of homogeneous draw the LDR should be equal to the MDR, unless mass is lost during drawing, for instance, by evaporation of remnants of solvent or degradation of the polymer. In this case the MDR should be greater than the LDR. However, in our case the MDR always appeared to be lower than the LDR. Sometimes deviations of more than 200% were obtained.

The LDR will appear to be greater than the MDR if (a) the mass of the fiber is inhomogeneously distributed over the fiber length, (b) the drawn fiber is wound elastically under high strain around the winding bobbin, or (c) inhomogeneous drawing takes place. To check whether the mass of the undrawn fiber was homogeneous, 2 m fiber was chopped in 2-cm pieces and weighted on a 7 decimal balance. The mass of the 2-cm pieces appeared to be constant within 5%, from which one may conclude that the fiber mass is homogeneously distributed over the fiber length. Elastical winding of the fiber could easily be verified by marking the fiber on the winding bobbin and

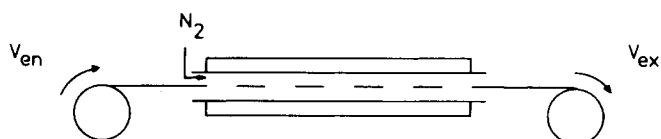


Fig. 3. Schematic presentation of a tube-drawing process.  $V_{en}$  = entrance velocity;  $V_{ex}$  = exit velocity of the fiber.

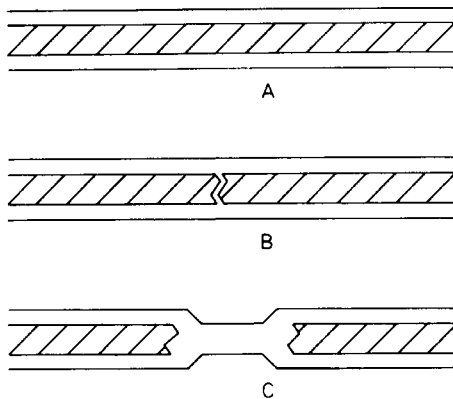


Fig. 4. Schematic presentation of a nonuniform draw induced by nonisothermal heating of the fiber.

measuring the length before and after rewinding the fiber. The length remained exactly the same (if elastical winding would occur only maximum deviations of about 20–25% could be obtained, which is the elongation at break as appears from the tensile tests). These observations indicated that inhomogeneous drawing<sup>24,25</sup> had taken place. Another observation was the impossibility of obtaining long continuous filaments without fracturing of the thread line in the hot-drawing tube.

These observations are likely to be due to a nonuniform heating of the fiber cross section.<sup>26</sup> As the fiber enters the drawing tube, it is heated and deformed simultaneously. Consequently, the outer layer of the fiber first reaches the drawing temperature, where the flow begins, while the inner core lies behind in temperature [Fig. 4(A)]. Under these circumstances thermal and compressive stress may be generated in the filament by the applied drawing stress. At a certain moment these stresses are high enough to fracture the inner core of the fiber [Fig. 4(B)] by way of voiding<sup>23,27,28</sup> and drawing proceeds by shearing of a concentric layer [Fig. 4(C)]. This nonuniform draw leads to variations in fiber diameter, until the fiber fractures which always seem to be in a thinner part of the fiber. The part of the fiber which is subsequently used in the stress-strain measurements has a diameter which is larger than expected on account of the LDR. For this reason the MDR always appeared to be lower than the LDR.

In the literature several techniques were used in order to overcome this nonisothermal drawing. High modulus polyoxymethylene fibers were produced by microwave heating and drawing,<sup>29–31</sup> in which it was possible to use the drawing stress effectively to orient the molecular chains in the noncrystalline regions of the polymer, because the noncrystalline regions were heated more effectively than the crystalline regions during dielectric heating. Kunugi and co-workers<sup>32,33</sup> used a zone-annealing method for drawing nylon 6 and poly(ethylene terephthalate) fibers, which has been very effective for extension and orientation of molecular chains, because a narrow portion of the fiber is heated under high tension and the heating zone moves with a constant speed in only one direction, changing the structure gradually and smoothly. An extension of this procedure is the hot-pin drawing process<sup>34,35</sup> in which

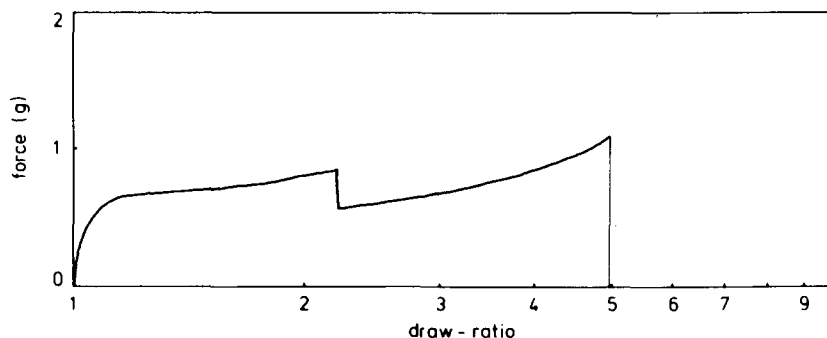


Fig. 5. Stress-strain curve for the elongation of a PLLA fiber using a deformation rate of  $4.445 \times 10^{-3} \text{ s}^{-1}$  and at a temperature of  $184^\circ\text{C}$  showing a drop in the force during the experiment (appears only incidentally).

only local heating is attempted in order to be able to use high tensions during drawing without getting inhomogeneous draw and without exposing the fiber to high temperatures for a long period.

If the supposedly nonuniform drawing mechanism of Figure 4 appears in the drawing tube during hot drawing, this phenomenon should not occur under isothermal conditions, unless the fiber skin deforms more easily than the inner core as a result of stress concentrations at the fiber surface.<sup>23</sup> For this reason an extensive investigation into the isothermal drawing of PLLA fibers seemed to be valuable. The advantage of using a dynamometer for these experiments was twofold. Not only isothermal conditions could be achieved, but also drawing could take place with a constant deformation rate, independent on the draw ratio. During the drawing experiments the axial tensile stress was recorded. Measurements were done in the temperature range from  $140$  to  $190^\circ\text{C}$  and with constant deformation rates in the range from  $0.444 \times 10^{-3}$  to  $8.889 \times 10^{-3} \text{ s}^{-1}$ . Using this range of deformation rates, self-heating of the samples due to internal friction<sup>36</sup> was essentially avoided.<sup>37</sup> Smook and Pennings<sup>37</sup> showed (for polyethylene fibers under identical experimental conditions) that the assumption of isothermal conditions was justified (within  $0.1^\circ\text{C}$ ) and no temperature increase, for example, as a result of adiabatic drawing,<sup>38</sup> happened. It was observed that, at temperatures above  $180^\circ\text{C}$  and using deformation rates larger than  $1.778 \times 10^{-3} \text{ s}^{-1}$ , during the experiment the force sometimes suddenly decreased (Fig. 5). By looking at the fiber at that moment we noticed that the drawing process was markedly nonuniform. In Figure 6 this nonuniform drawing under isothermal conditions is schematically represented. Starting the experiment, the fiber is drawn homogeneously over the entire sample length [Figs. 6(A) and 6(B)]. At the moment the force drops a neck forms [Fig. 6(C)], whereafter the neck runs in the direction of the fiber ends, leading to relaxation of the thicker parts of the fiber until the fiber fractures. This phenomenon appeared only incidentally at temperatures in the range of  $180$ – $190^\circ\text{C}$  and using deformation rates larger than  $1.778 \times 10^{-3} \text{ s}^{-1}$ . Obviously, even under isothermal conditions, at high deformation rates the negative hydrostatic pressure is high enough to induce inhomogeneous drawing. Figure 7 presents a SEM micrograph of the neck formed during isothermal drawing at a constant deformation rate.

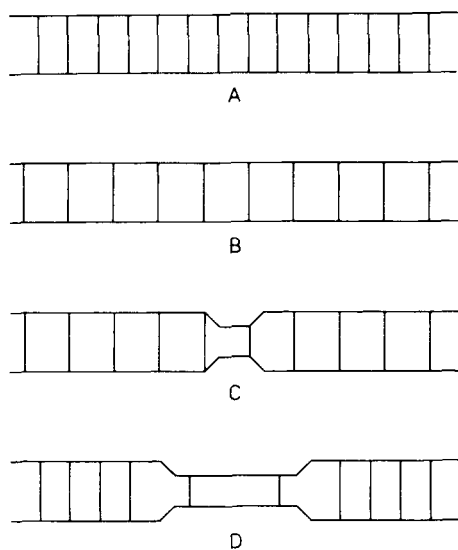


Fig. 6. Schematic presentation of a nonuniform drawing under isothermal conditions as incidentally observed in the dynamometer at temperatures above  $180^{\circ}\text{C}$  and using deformation rates larger than  $1.778 \times 10^{-3} \text{ s}^{-1}$ , showing relaxation of some parts of the fiber and elongation of other parts.

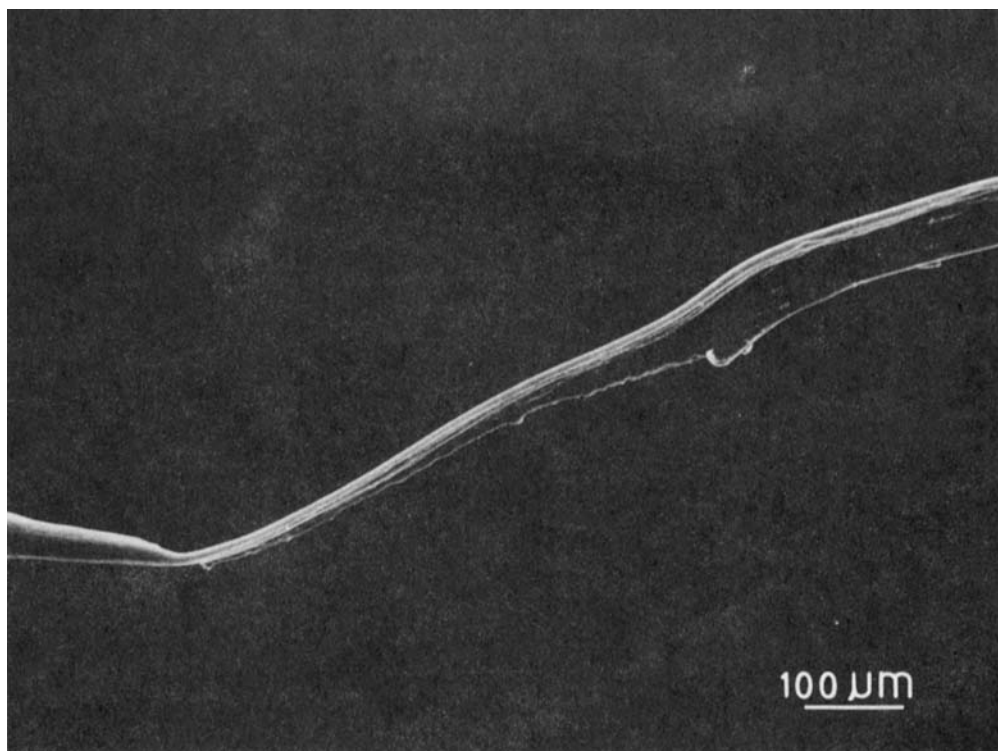


Fig. 7. SEM micrograph of a neck formed during isothermal drawing at a constant deformation rate.



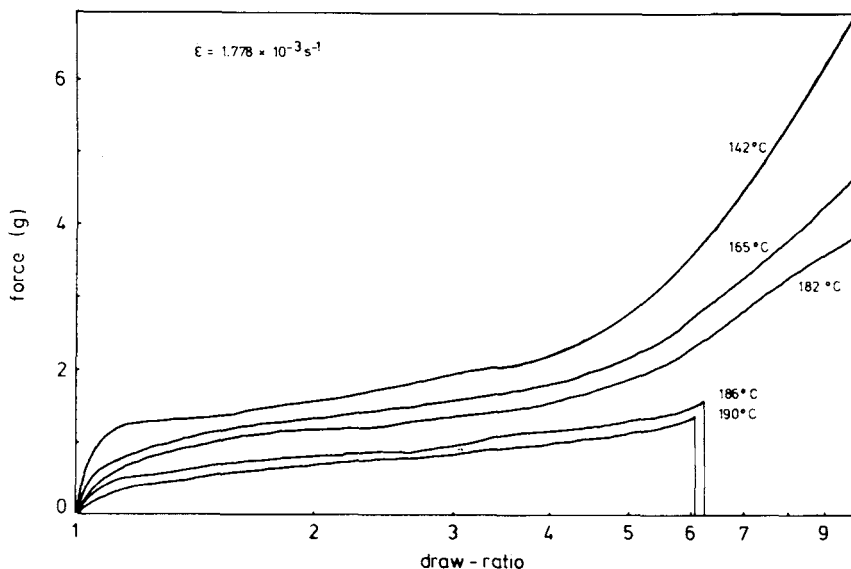


Fig. 8. Stress-strain curves for the elongation of PLLA fibers at different temperatures using a deformation rate of  $1.778 \times 10^{-3} \text{ s}^{-1}$ .

In Figure 8 the experimental stress-strain curves are presented. They were obtained by applying a deformation rate of  $1.778 \times 10^{-3} \text{ s}^{-1}$  at different drawing temperatures. It shows that the drawing behavior is very sensitive to the drawing temperature. At low drawing temperatures, i.e., 140–180°C, the force rapidly increases at draw ratios larger than 4 as a result of strain hardening by fibrillar crystallization of partially extended chains. A draw ratio of 10 is the experimental limit of the dynamometer. In the temperature range between 180 and 190°C, this experimental limit could not be obtained. According to the elongational flow theory,<sup>27,39</sup> drawing will only proceed effectively if the orientation action of the flow field prevails over the relaxation phenomena, e.g., Brownian motion. This is expressed in the following condition:

$$\dot{\epsilon} \cdot \tau_r > 1 \quad (3)$$

where  $\dot{\epsilon}$  is the deformation rate and  $\tau_r$  is a characteristic relaxation time of the material. As the molecules become more extended the tendency to recoil will grow stronger. Apparently a deformation rate of  $1.778 \times 10^{-3} \text{ s}^{-1}$  is too small to induce fibrillar crystallization, and at a certain stage of the drawing process the relaxation phenomena starts to dominate and the fiber fractures.<sup>37,40-44</sup>

The elongational viscosity can be determined by the equation

$$\eta_e = \sigma_x / \dot{\epsilon} \quad (4)$$

where  $\sigma_x = F_x / A_x =$  axial tensile stress,  $F_x =$  axial tensile force,  $A_x =$  cross section of the fiber at place  $x$ , and  $\dot{\epsilon} = \delta V_x / \delta x =$  deformation rate in the direction of the fiber axis (= constant). Using relation (4), in Figure 9, the

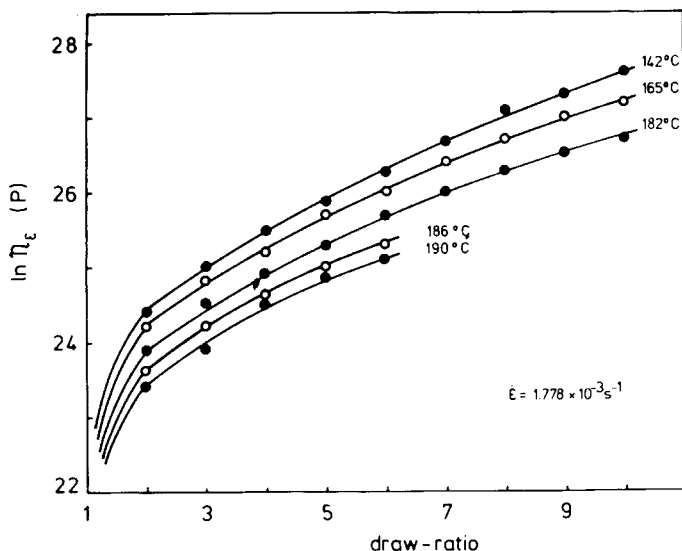


Fig. 9. Elongational viscosity ( $\eta_e$ ) vs. draw ratio upon drawing PLLA at various temperatures using a deformation rate of  $1.778 \times 10^{-3} \text{ s}^{-1}$ .

$\ln \eta_e$  is presented as a function of the draw ratio for different temperatures at a deformation rate of  $1.778 \times 10^{-3} \text{ s}^{-1}$ . Remarkably high viscosities were measured between  $10^9$  and  $10^{12}$  (1 P = 0.1 Pa s). These viscosities were in the same range as the ones measured by Smook and Pennings<sup>37</sup> for ultrahigh molecular weight polyethylene fibers, although the PLLA has a lower molecular weight and a higher chain flexibility.<sup>45</sup> The elongational viscosity decreases going to higher temperatures but increases during the drawing experiment.

Calculation of the elongational viscosities from the experimental curves at a constant temperature of  $175^\circ\text{C}$  resulted in the graphs of Figure 10, demonstrating an increase in elongational viscosity with draw ratio. Higher deformation rates resulted in higher elongational viscosities, which is in line with theoretical predictions<sup>40-44</sup>; although studies on other polymers reported that  $\eta_e$  can increase, decrease, or even remain constant with increasing deformation rates.<sup>46</sup> For instance, steady state viscosity data on high density polyethylene and polypropylene showed a decreasing value of  $\eta_e$  with deformation rate.<sup>47</sup>

For the elongational viscosity a thermally activated process can be expected, according to the Eyring-Frenkel equation<sup>48</sup>

$$\eta_e(T) = \eta_e(T_0) \exp \left[ \frac{E_a}{R} \left( \frac{1}{T} - \frac{1}{T_0} \right) \right] \quad (5)$$

where  $E_a$  is the apparent activation energy and  $R$  is the gas constant. The activation energy of the drawing process  $E_a$  as determined from the dependence of  $\ln \eta_e$  on  $T^{-1}$  will give information concerning the nature of the deformation process.<sup>37,49,50</sup> Figures 9 and 10 indicate that  $\eta_e$  is strongly affected by the draw ratio as well as the deformation rate. For this reason it is necessary to compare  $\eta_e$  at a fixed value of the draw ratio  $\lambda$  and  $\dot{\epsilon}$  at each temperature to get a proper estimate of the activation energy. In Figure 11

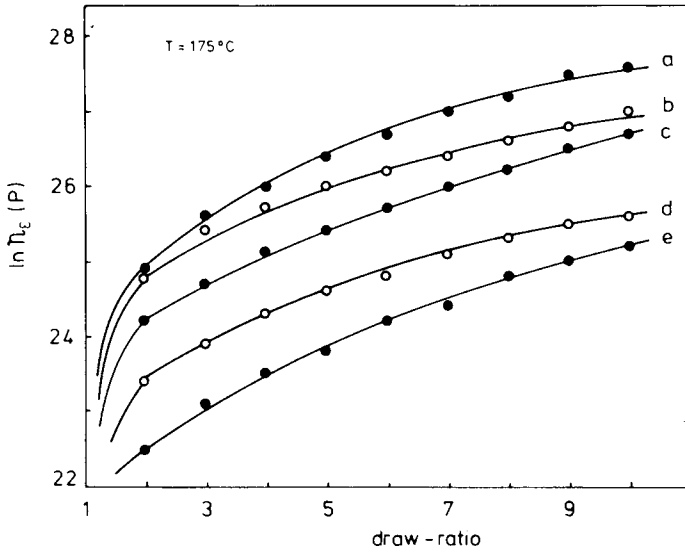


Fig. 10. Elongational viscosity ( $\eta_e$ ) vs. draw ratio upon drawing PLLA at 175°C with different deformation rates  $\dot{\epsilon}$  ( $\text{s}^{-1}$ ): (a)  $0.444 \times 10^{-3}$ ; (b)  $0.889 \times 10^{-3}$ ; (c)  $1.778 \times 10^{-3}$ ; (d)  $4.445 \times 10^{-3}$ ; (e)  $8.889 \times 10^{-3}$ .

$\ln \eta_e$  is plotted against  $T^{-1}$  for several draw ratios. Two different temperature regions were observed for all values of  $\lambda$  characterized by a linear relation of  $\ln \eta_e$  vs.  $T^{-1}$ . One region of low activation energy up to 180°C and one region of high activation energy in the temperature range between 180 and 190°C.

Figure 12 presents the activation energies for the two different temperature regions, as calculated from the slope of the straight lines in Figure 11, as a

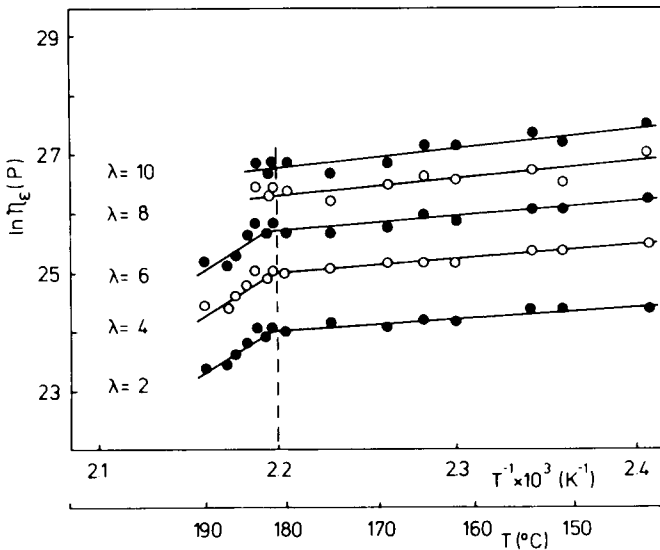


Fig. 11. Plot of the logarithm of the elongational viscosity ( $\ln \eta_e$ ) vs. reciprocal temperature ( $T^{-1}$ ) at several draw-ratios for the determination of the activation energy.

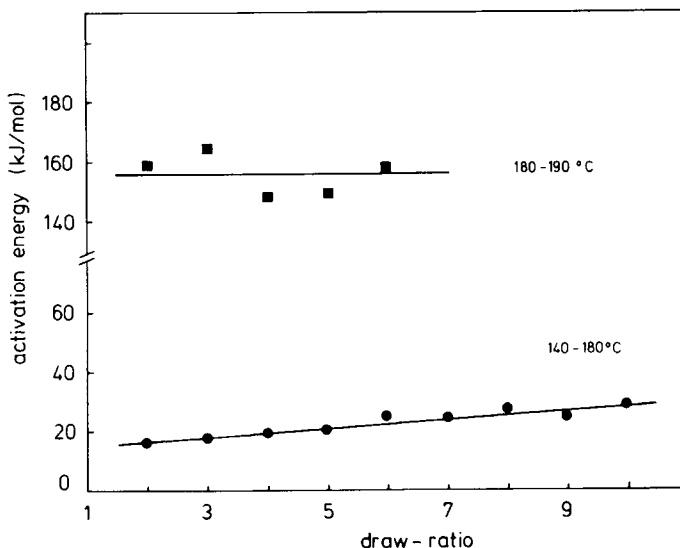


Fig. 12. Activation energies as a function of draw ratio for two temperature regions.

function of draw ratio. In the lowest temperature region (up to 180°C) the activation energy increases only slightly from 15 kJ/mol for  $\lambda = 2$ –28 kJ/mol for  $\lambda = 10$ . An  $\alpha, \beta$  transition of the PLLA at higher draw ratios has not been observed. In the region between 180 and 190°C activation energies were found to vary from 145 to 165 kJ/mol. The dispersion of the measurements has to be ascribed to very little nonuniform deformation as mentioned earlier. For polyethylene fibers, three intervals of different activation energies were distinguished.<sup>37</sup> In the temperature range between 100 and 130°C [below the melting temperature of the undrawn sample<sup>51</sup>] hot drawing proceeds presumably by a sliding motion of separated fibrillar units. Between 133 and 143°C partial melting at the surface of the fibrils caused aggregation of the elementary fibrils. Above 143°C molecular orientation was achieved accomplished by slippage of individual molecules through the crystal lattice and the release of stress concentrations by the rapid transport of Reneker point defects<sup>52</sup> along the chains. In this region the entanglements may act as semipermanent crosslinks providing the necessary coherence between the molecules.<sup>53</sup> In this temperature range the activation energy was dependent on draw ratio.

Valuable information about the origin of the deformation process of PLLA in the two temperature regions is obtained from the shrinkage ( $S$ ) of the fiber after releasing the stress which is built up during the hot-drawing experiment. This shrinkage, which is a measure of the permanent deformation during the hot drawing, is defined as

$$\text{shrinkage } (S) = \left( \frac{l_1 - l_2}{l_1} \right) \times 100\% \quad (6)$$

where  $l_1$  = the length of the fiber after the hot-drawing experiment, which always was taken  $10 \times l_0$  ( $l_0$  = initial fiber length), and  $l_2$  = the length of the fiber at the moment that the axial tensile force is reduced to zero, when the

TABLE I  
Shrinkage of the Fiber after Releasing the Stress at Various Temperatures and Using  
a Deformation Rate of  $1.778 \times 10^{-3} \text{ s}^{-1}$

Temperature (°C)	Shrinkage (%)	
142.0	12	Region I
151.3	12	
153.5	12	
161.0	13	
165.0	12	
180.0	31	Region II
181.7	29	
182.5	53	
183.6	47	
Higher	Fracture	

distance between the fiber ends was reduced in order to lower the axial tensile force. In Table I the shrinkage of the fiber is presented for different temperatures after hot drawing with a deformation rate of  $1.778 \times 10^{-3} \text{ s}^{-1}$ . In the temperature region up to  $180^\circ\text{C}$  (low activation energy region) the shrinkage of the fiber after releasing the stress always appeared to be in the range of 12–13%, which indicates that in this region the deformation proceeds in the semicrystalline state of the polymer. In the temperature region between  $180$  and  $190^\circ\text{C}$  (region of high activation energy) the shrinkage appeared to be 30% or higher. It seems to be that in this region the deformation proceeds in the semiliquid state of the polymer (the melting temperature of the undrawn sample was  $179^\circ\text{C}$ ). Releasing the stress caused relaxation of the chains to a random configuration. In Table II the shrinkage is presented as a function of deformation rate and temperature. Obviously the shrinkage is independent on the deformation rate in the low temperature range. At temperatures above  $180^\circ\text{C}$  a draw ratio of 10 could not be achieved at low deformation rates because of the insufficient strain hardening, and at very high deformation rates because of the inhomogeneous drawing leading to premature fracturing of the filament.

During the hot drawing under nonisothermal conditions the fiber is guided through a glass tube (Fig. 3) in which a temperature gradient (Fig. 13) is

TABLE II  
Shrinkage of the Fiber after Releasing the Stress at Various Temperatures  
as a Function of Different Deformation Rates<sup>a</sup>

Deformation rate ( $\text{s}^{-1}$ )	$T$ (°C)				
	151.3	161	180	182	183.6
$0.444 \times 10^{-3}$	11%	18%	—	—	—
$0.778 \times 10^{-3}$	8%	20%	42%	—	—
$1.778 \times 10^{-3}$	12%	13%	31%	53%	47%
$4.445 \times 10^{-3}$	17%	15%	47%	55%	—
$8.889 \times 10^{-3}$	17%	17%	47%	67%	—

<sup>a</sup>(For the missing values a draw ratio of 10 could not be achieved)

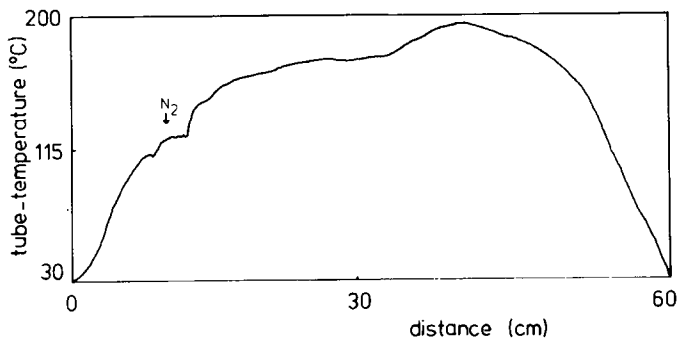


Fig. 13. Temperature in the drawing tube at different positions in the tube, showing a temperature gradient, induced by the nitrogen inlet and entrance/exit effects.

introduced by the nitrogen inlet and entrance/exit effects. In the tube the fiber itself is exposed to a temperature gradient too and the deformation mechanism will depend on the place in the tube (the temperature). Using a hot-spot temperature of  $190^{\circ}\text{C}$  it is possible for each deformation rate to estimate the draw ratio of the fiber at the various tube temperatures. Using the axial tensile force at break of the fiber at  $190^{\circ}\text{C}$ , the draw ratio which the fiber had obtained at that specific axial tensile force at the other temperatures is determined. The values are shown in Figure 14 for different deformation rates. It shows that using deformation rates larger than  $1.778 \times 10^{-3} \text{ s}^{-1}$  high draw ratios were already obtained at low tube temperatures, while using deformation rates of  $1.778 \times 10^{-3} \text{ s}^{-1}$  or lower the drawing proceeds mainly above  $180^{\circ}\text{C}$ . This indicates that at high deformation rates the drawing takes place in the semicrystalline state, in which presumably crystal blocks will be deformed by shear deformation, while at low deformation rates the drawing

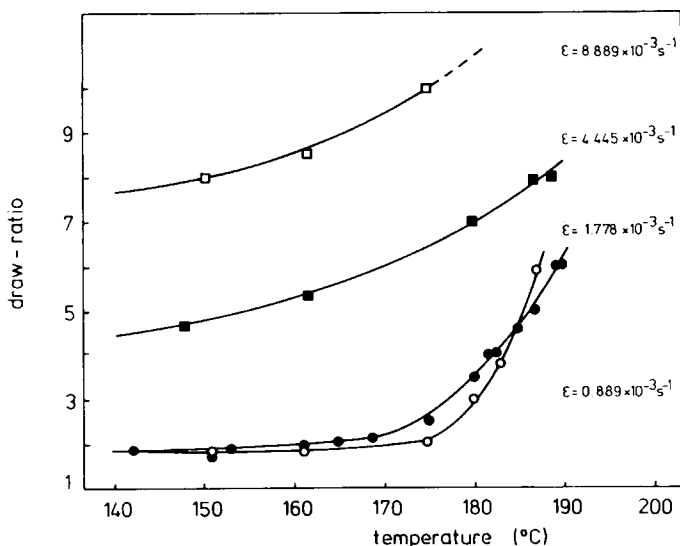


Fig. 14. Draw ratio of a fiber at various deformation rates vs. temperature in a tube-drawing process.

proceeds in the semiliquid state of the PLLA leading to a homogeneous draw at a molecular level. Using the low deformation rate the tube drawing strongly resembles the hot-pin and zone-heating processes.<sup>32-35</sup> During deformation in the semicrystalline state the crystalline as well as the noncrystalline regions have to be deformed simultaneously.<sup>54</sup> This can only optimally happen if both the temperature and the deformation rate have been optimized.<sup>55</sup> Transport of chains or parts of chains through the lattice will scarcely occur, resulting in almost no removal of topological defects like entanglements and intertwinings. In the case of polyethylene fibers the drawing is less accessible for the unique combination of the deformation rate and temperature, because drawing of these low-entanglement-density fibers easily occurs by crazing and multiple yielding.<sup>23,56</sup> However, polymers with more inter and intramolecular interactions like polyoxymethylene<sup>54</sup> and PLLA seem to be very susceptible for this phenomenon. This process seems also to be depending on the molecular weight and molecular weight distribution.<sup>54</sup> By deformation in the liquid state of the PLLA, these problems are circumvented, because the drawing proceeds by deformation of a noncrystalline network in which individual molecules can easily be aligned and the development of stress concentrations by shear-deformation will be suppressed<sup>37</sup> by the rapid transport of Reneker<sup>52,57</sup> defects. The entanglements will slip off into newly created disordered domains, and fibrillar crystallization can take place properly. Figure 14 shows that during tube drawing this liquid-state drawing can only be achieved by applying low deformation rates.

The appearance of the nonuniform draw at high deformation rates, most likely induced by thermal and compressive stresses, and the knowledge of the existence of two drawing regions suggests that drawing should be performed at very low deformation rates (or, in the case of tube drawing, low entrance velocities). Using low entrance velocities isothermal drawing conditions can be

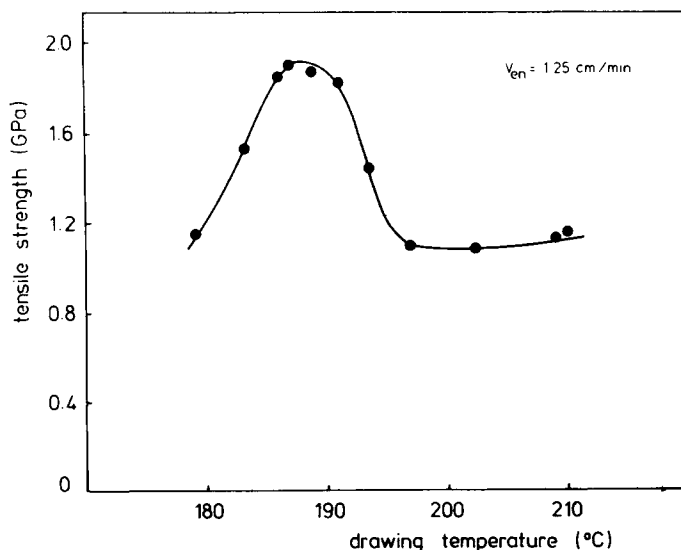


Fig. 15. Tensile strength of PLLA fibers hot-drawn at different temperatures to the maximal draw ratio using an entrance velocity of 1.25 cm/min in a tube-drawing process.

approached. Reperforming the hot drawing experiments using an entrance velocity of 1.25 cm/min revealed a completely changed relation between the hot-drawing temperature and the ultimate tensile strength after hot drawing to the maximum draw ratio. Figure 15 presents the ultimate tensile strength as a function of the drawing temperature. A maximum in tensile strength of 2.0 GPa was achieved after drawing at 188°C to a maximum draw ratio of 13. Remarkably, this ultimately attainable draw ratio of 13 calculated from the increase in length (LDR) was exactly the same as the LDR attained after using an entrance velocity of 6.25 cm/min, except at this time the LDR appeared always within 5% the same as the MDR, indicating that uniform drawing had been attained. The low values of the draw ratio, leading to excellent fiber properties, indicate that, although the entanglements are mobile enough to slip off into newly created disordered domains, disentangling is impeded by the rapid formation of fibrillar crystals between the entanglement-rich domains. Another observation was that, using a low entrance velocity, long continuous filaments could be obtained.

Reducing the deformation rate and thus the drawing stress can also be achieved by using a two-step drawing process. Clark and Scott<sup>58</sup> produced high-strength polyoxymethylene fibers by first drawing at elevated temperatures to the "natural draw ratio" and then at a very slow rate (5%/min) to the ultimate draw ratio. Two-stage drawing experiments on PLLA were performed by drawing the PLLA fiber in the first stage to  $\lambda = 3$  in three different ways: at room temperature, at 85°C (above  $T_g$ ), and at 190°C, followed by drawing in the second stage at a temperature of 190°C or 214°C. In all cases this two-stage drawing of PLLA resulted in moderate mechanical properties. This seems to demonstrate not only that the deformation rate is responsible for the ultimate mechanical properties, but also that a harmonization of drawing temperature and deformation rate is needed for every selected

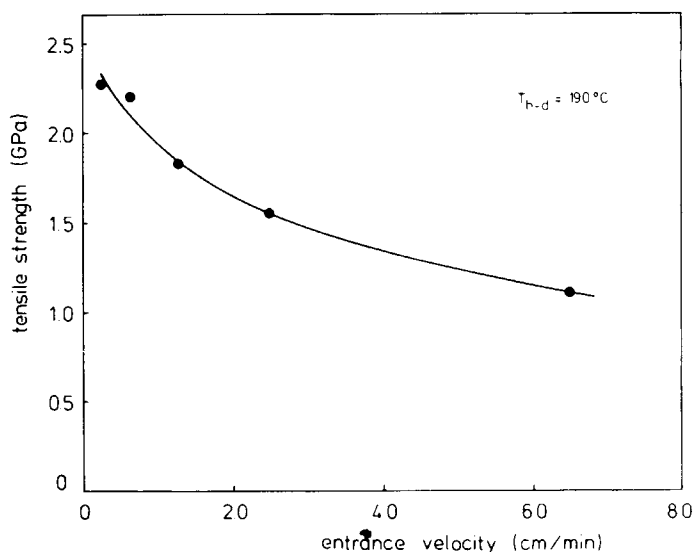


Fig. 16. Tensile strength of PLLA fibers after hot drawing at 190°C to the maximal draw ratio as a function of the entrance velocity.



molecular weight and molecular weight distribution in order to achieve the correct drawing conditions leading to the ultimate mechanical properties. Brew and Ward<sup>54</sup> found for polyoxymethylene fibers that high draw and high modulus could only be obtained within a very narrow window of temperature and strain rates. They suggested that this is because both the crystalline and noncrystalline materials are involved in the deformation process and that there must be a coincidence of rates for the two processes to occur simultaneously. This prevents any simple combination of strain rate and temperature being an adequate condition for drawing, so that drawing at high rates and temperatures is not equivalent to drawing at low rates and low temperatures. In Figure 16 the ultimate tensile strength of the PLLA fibers is shown after hot drawing at 190°C to the maximum draw ratio as a function of entrance velocity. In all cases the LDR appeared to be 13, while the MDR diverged mostly at high entrance velocities. PLLA fibers with a tensile strength of 2.3 GPa were achieved after hot drawing at 190°C using an entrance velocity of

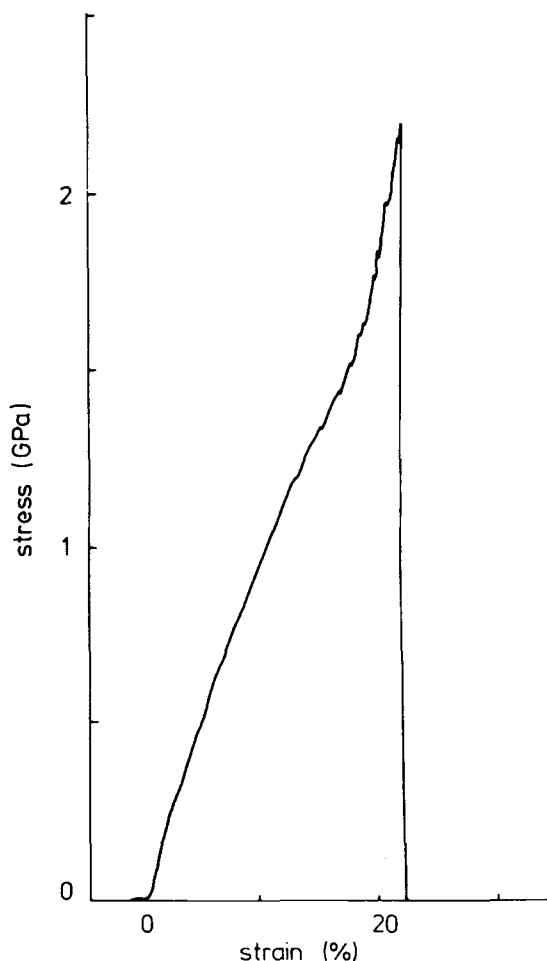


Fig. 17. Stress-strain curve of a high strength PLLA fiber after drawing at 190°C using an entrance velocity of 0.625 cm/min, showing an upturn at high strain.

0.625 cm/min. The residence time in the tube was about 75 min. This long a period of time is not harmful as long as the stresses are low. Lower entrance velocities resulted in fiber fracture caused by the insufficient orientation action in the drawing process.

Figure 17 presents a stress-strain curve of a high-strength PLLA fiber. Remarkably, at high strain the modulus increases, indicating that just prior to fracture the fiber is capable of absorbing an extra amount of energy, most probably originating from the  $\alpha, \beta$  crystal transition.<sup>13</sup> This upturn of the stress-strain curve only takes place for the fibers drawn under optimal conditions.

## CONCLUSIONS

Summarizing the results, we come to the conclusion that the hot drawing of PLLA fibers can take place in two temperature regions. One region up to 180°C, in which deformation takes place in the semicrystalline state of the polymer, and one region between 180 and 190°C in which the deformation proceeds in the liquid state of the polymer, leading to a semicrystalline state by strain hardening after displacement of topological defects. If high deformation rates are applied during tube drawing, the deformation will principally proceed in the semicrystalline region, probably by shear deformation, and inhomogeneous draw will take place, leading to inferior fiber properties, unless the deformation rate and temperature are strictly adjusted. This process seems to be depending on molecular weight and molecular weight distribution.

Homogeneous drawing can be achieved by using low deformation rates so that the deformation may take place in the semiliquid state of the PLLA in which individual chains can easily be aligned and topological defects can be removed. PLLA fibers with a tensile strength of 2.3 GPa can be produced in this way.

One of the authors (A. R. P.) wishes to acknowledge the AKZO Research Department, The Netherlands, for financial support. The authors also wish to express their gratitude to H. v. d. Wolf for his assistance in the experimental work. H. Nijland is acknowledged for the SEM photographs and A. B. Verwey for providing the PLLA sample.

## References

1. R. W. Postlethwait, *Arch. Surg.*, **101**, 489 (1970).
2. D. E. Cutright and E. E. Hunsuck, *Oral. Surg.*, **31**, 134 (1971).
3. A. K. Schneider, U.S. Pat. 3.636,956 (1972); *Chem. Abstr.*, **66**, 56510w (1967).
4. B. Eling, S. Gogolewski, and A. J. Pennings, *Polymer*, **23**, 1587 (1982).
5. S. Gogolewski and A. J. Pennings, *J. Appl. Polym. Sci.*, **28**, 1045 (1983).
6. S.-H. Hyon, K. Jamshidi, and Y. Ikada, *Polym. Prep.*, **24**, 6 (1983).
7. S. Syamala Devi and P. J. Vasudevan, *Macromol. Chem. Phys.*, **25**, 315 (1985).
8. J. W. Leenslag, S. Gogolewski, and A. J. Pennings, *J. Appl. Polym. Sci.*, **29**, 2829 (1984).
9. J. W. Leenslag and A. J. Pennings, *Polymer*, **28**, 1695 (1987).
10. M. Vert, P. Christel, F. Chabot, and L. Leray, in *Macromolecular Biomaterials*, G. W. Hastings and P. Ducheyne, Eds., CRC Press, Boca Raton, FL 1984, Chap. 6, p. 120.
11. J. W. Leenslag, A. J. Pennings, R. P. H. Veth, H. K. L. Nielsen, and H. W. B. Jansen, *Macromol., Rapid Commun.*, **5**, 815 (1985).
12. B. E. Cohan, J. W. Leenslag, J. Miles, and A. J. Pennings, *Arch. Ophthalmol.*, **103**, 1816 (1985).
13. W. Hoogsteen, G. ten Brinke, and A. J. Pennings, to appear.

14. G. Capaccio and I. M. Ward, *Polym. Eng. Sci.*, **15**, 219 (1975).
15. G. Capaccio and I. M. Ward, *Polymer*, **16**, 239 (1975).
16. G. Capaccio, T. A. Crompton, and I. M. Ward, *J. Polym. Sci., Polym. Phys. Ed.*, **14**, 1641 (1976).
17. G. Capaccio, A. G. Gibson, and I. M. Ward, in *Ultra High Mod. Pol.*, A. Ciferri and I. M. Ward, Eds., Applied Science, London, 1979, Chap. 1.
18. P. G. de Gennes, *Macromolecules*, **17**, 703 (1984).
19. J. W. Leenslag and A. J. Pennings, *Macromol. Chem.*, **188**, 1809 (1987).
20. A. Schindler and D. Harper, *J. Polym. Sci., Polym. Chem. Ed.*, **17**, 2593 (1979).
21. E. W. Fisher, H. J. Sterzel, and G. Wegner, *Kolloid Z. Z. Polym.*, **251**, 980 (1973).
22. A. Posthuma de Boer and A. J. Pennings, *Macromolecules*, **10**, 981 (1977).
23. A. R. Postema, P. Smith, G. O. R. Alberda van Ekenstein, and A. J. Pennings, to appear.
24. A. Peterlin, *Polym. Eng. Sci.*, **17**, 183 (1977).
25. R. H. Butler, D. C. Prevorsek, and Y. D. Kwon, *Polym. Eng. Sci.*, **22**, 329 (1982).
26. J. Smook, W. Hamersma, and A. J. Pennings, *J. Mater. Sci.*, **19**, 1359 (1984).
27. A. Ziabicki, *Fundamentals of Fibre Formation*, Wiley, London, 1976, Chap. 6.
28. D. C. Hookway, *J. Text. Inst.*, **49**, P292 (1958).
29. K. Nakagawa, O. Maeda, and S. Yamakawa, *J. Polym. Sci., Polym. Lett. Ed.*, **21**, 933 (1983).
30. Y. Takeuchi, F. Yamamoto, and K. Nakagawa, *J. Polym. Sci., Polym. Phys. Ed.*, **23**, 1193 (1985).
31. K. Nakagawa, T. Konaka, and S. Yamakawa, *Polymer*, **26**, 84 (1985).
32. T. Kunugi, T. Ikuta, M. Hashimoto, and K. Matsuzaki, *Polymer*, **23**, 1983 (1982).
33. T. Kunugi, A. Suzuki, and M. Hashimoto, *J. Appl. Polym. Sci.*, **26**, 213 (1981).
34. V. A. Marichin, L. P. Mjasnikova, D. Zenke, R. Hirte, and P. Wiegel, *Polym. Bull.*, **12**, 287 (1984).
35. A. V. Savitski, I. A. Gorshkova, I. L. Frolova, G. N. Shmikk, and A. Loffe, *Polym. Bull.*, **12**, 195 (1984).
36. A. Peterlin, *J. Mater. Sci.*, **6**, 490 (1971).
37. J. Smook and A. J. Pennings, *J. Appl. Polym. Sci.*, **27**, 2209 (1982).
38. I. Marshall and A. B. Thompson, *Proc. Roy. Soc. London Ser. A*, **221**, 541 (1954).
39. G. Marrucci, *Polym. Eng. Sci.*, **15**, 229 (1975).
40. M. Yamamoto, *J. Phys. Soc. Jpn.*, **12**, 1148 (1957).
41. A. S. Lodge, *Elastic Liquids*, Academic, New York, 1964.
42. J. L. White, *J. Appl. Polym. Sci.*, **8**, 1129 (1964).
43. M. C. Williams and R. B. Bird, *Phys. Fluids*, **5**, 1126 (1962).
44. T. W. Spriggs, *Chem. Eng. Sci.*, **20**, 931 (1965).
45. A. E. Tonelli and P. J. Flory, *Macromolecules*, **2**, 225 (1969).
46. J. L. White, *Appl. Polym. Symp.*, **33**, 31 (1978).
47. Y. Ide and J. L. White, *J. Appl. Polym. Sci.*, **22**, 1061 (1978).
48. C. D. Han and R. R. Lamonte, *Trans. Soc. Rheol.*, **16**, 447 (1972).
49. A. Peterlin, *Fracture*, **1**, 471 (1977).
50. W. T. Mead and R. S. Porter, *J. Polym. Sci., Polym. Symp.*, **63**, 289 (1978).
51. J. Smook and A. J. Pennings, *Coll. Polym. Sci.*, **262**, 712 (1984).
52. D. H. Reneker, *J. Polym. Sci.*, **59**, 539 (1962).
53. L. Fisher, R. Harschberger, A. Ziegeldorf, and W. Ruland, *Coll. Polym. Sci.*, **260**, 174 (1980).
54. B. Brew and I. M. Ward, *Polymer*, **19**, 1338 (1978).
55. A. B. Thompson, in *Fiber Structure*, J. W. S. Hearle and R. H. Peters, Eds., Text. Inst. Butterworths, London, 1963, p. 511.
56. T. Juska and I. R. Harrison, *Polym. Eng. Rev.*, **2**, 13 (1982).
57. D. H. Reneker and J. Mazur, *Polymer*, **25**, 1549 (1984).
58. E. S. Clark and L. S. Scott, *Polym. Eng. Sci.*, **14**, 682 (1974).

Received February 16, 1988

Accepted May 12, 1988